Supplemental Figure 1

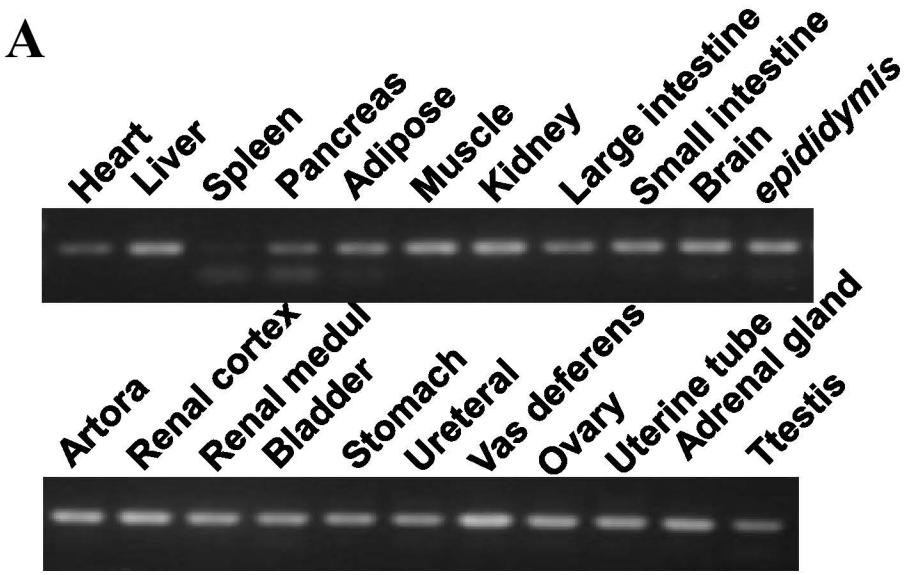

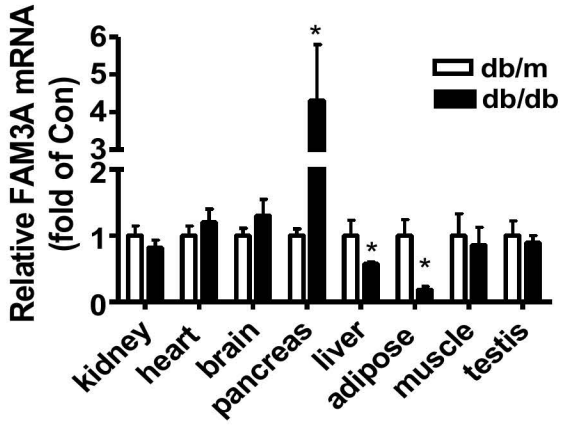

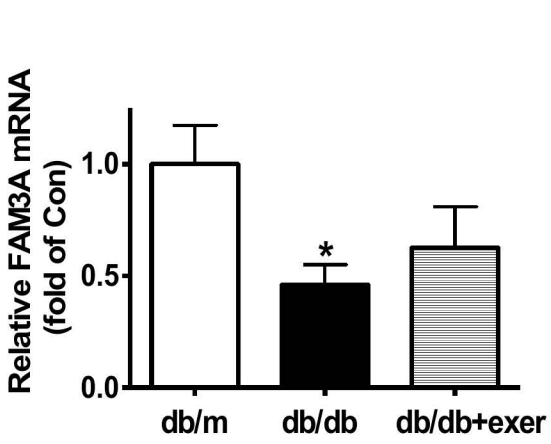

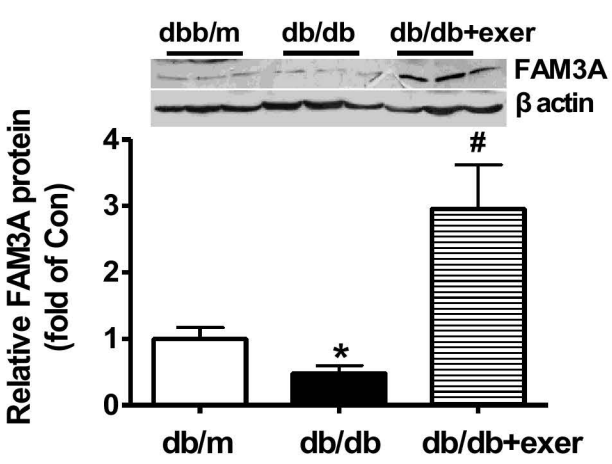

Supplemental Figure 10

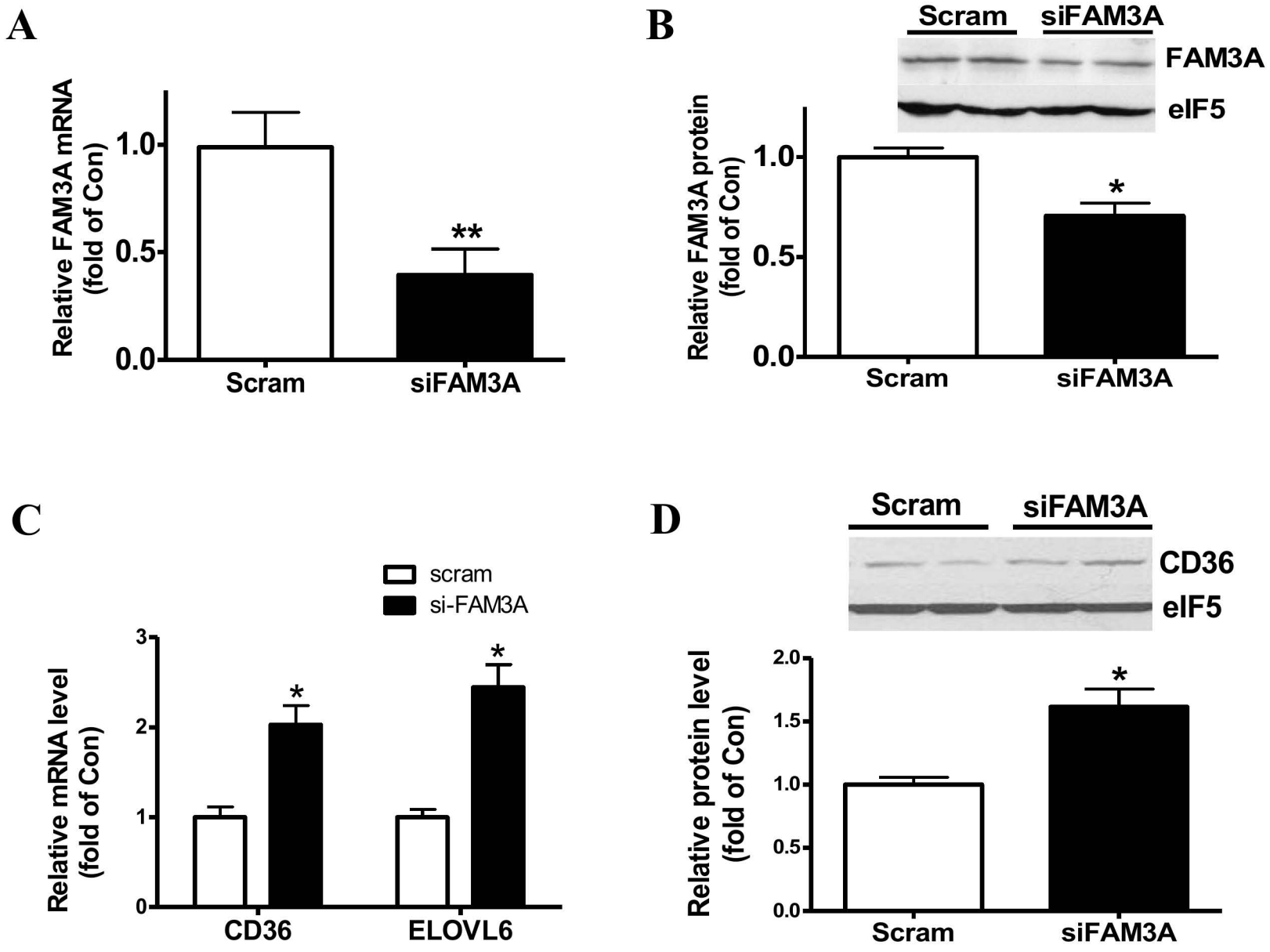

Supplemental Figure 11

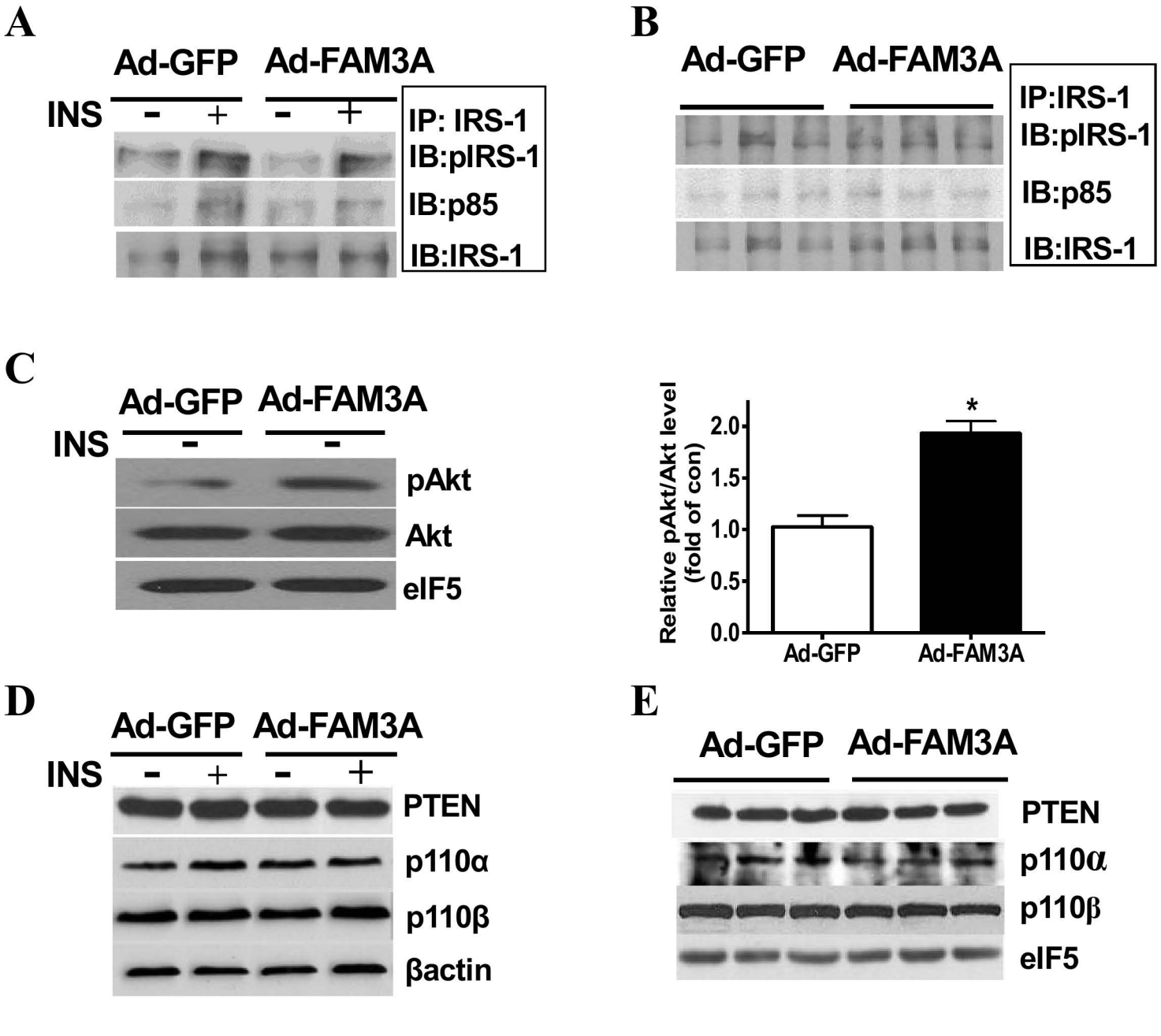

Supplemental Figure 12

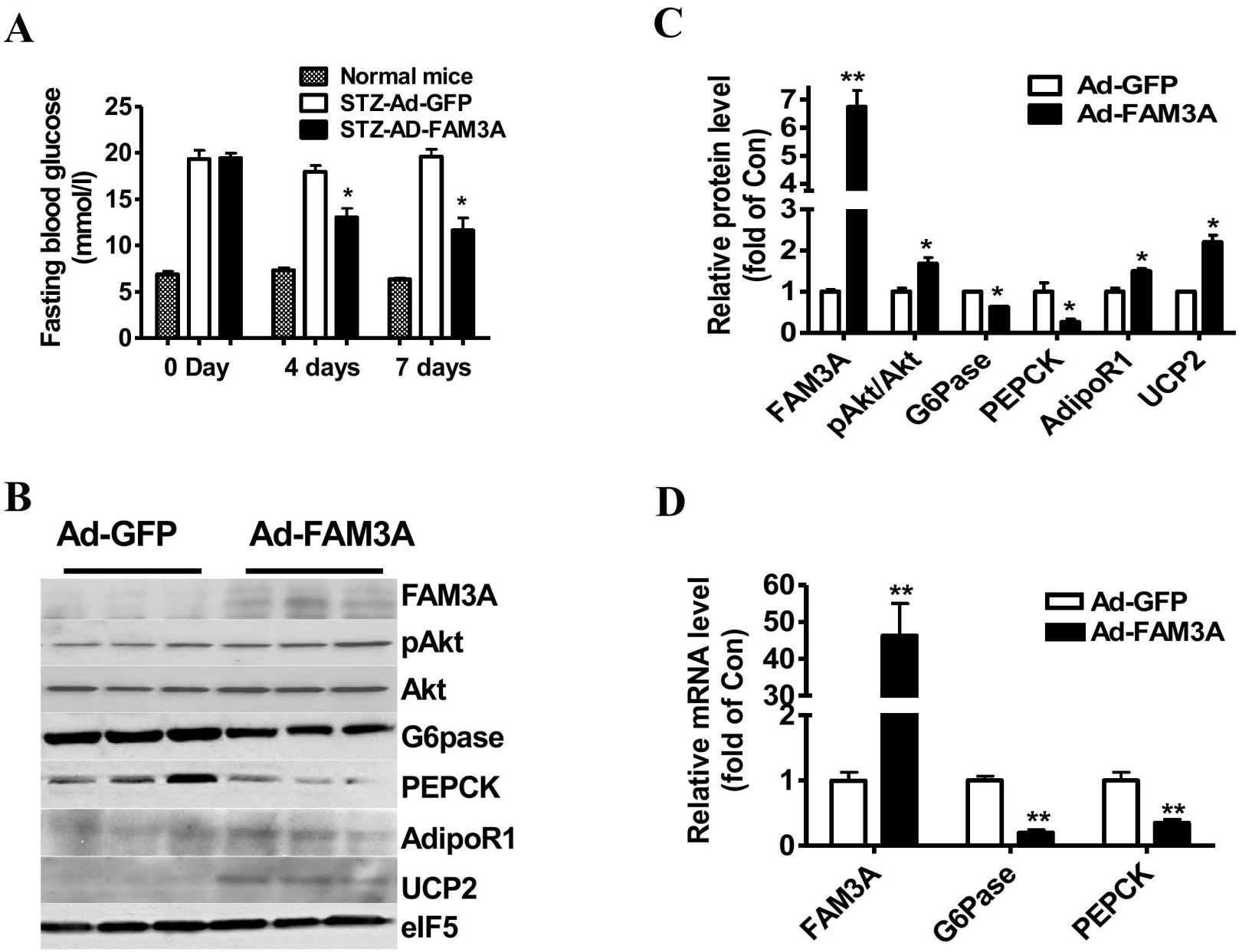

Supplemental Figure 13

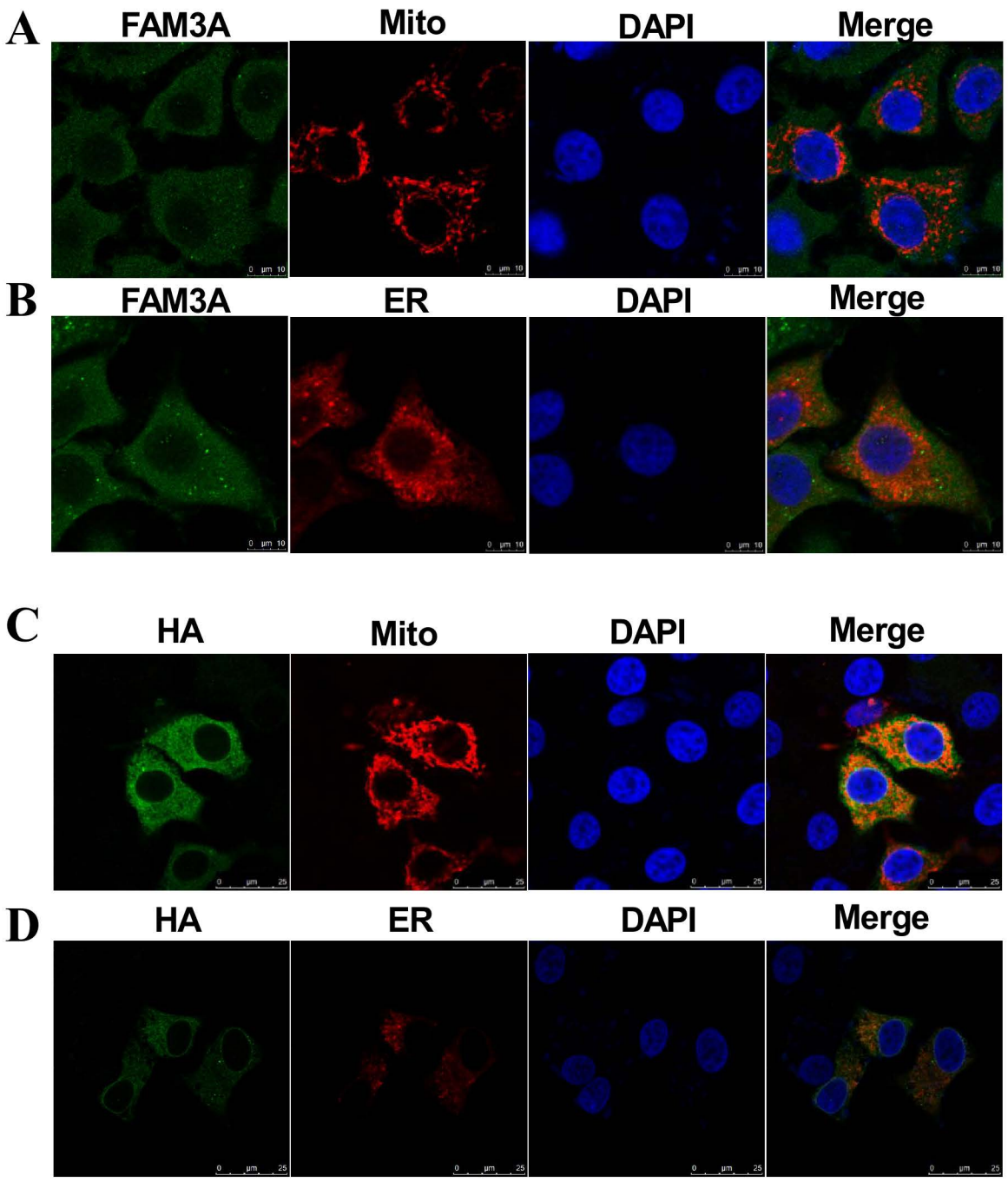

Supplemental Figure 14

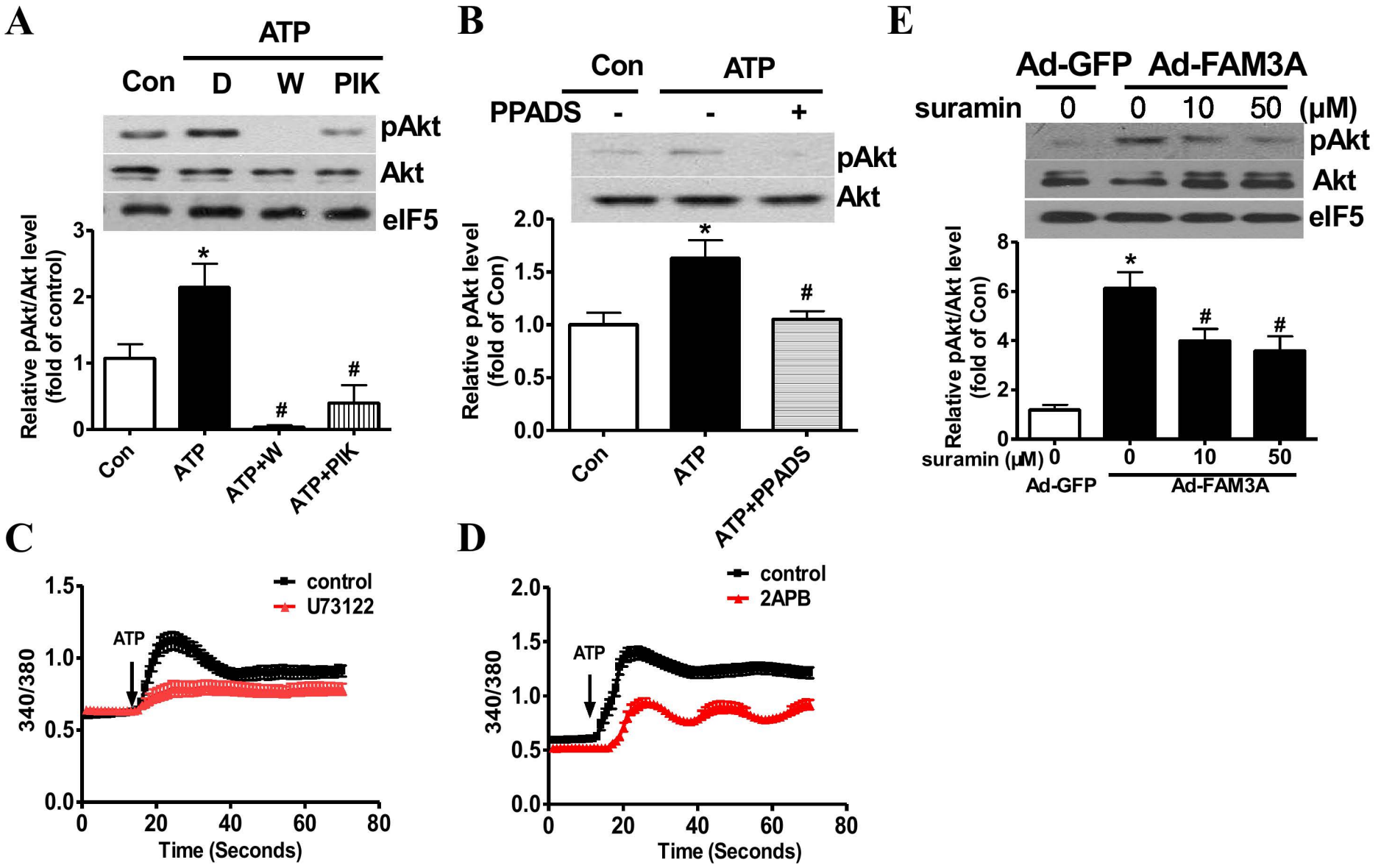

Supplemental Figure 15

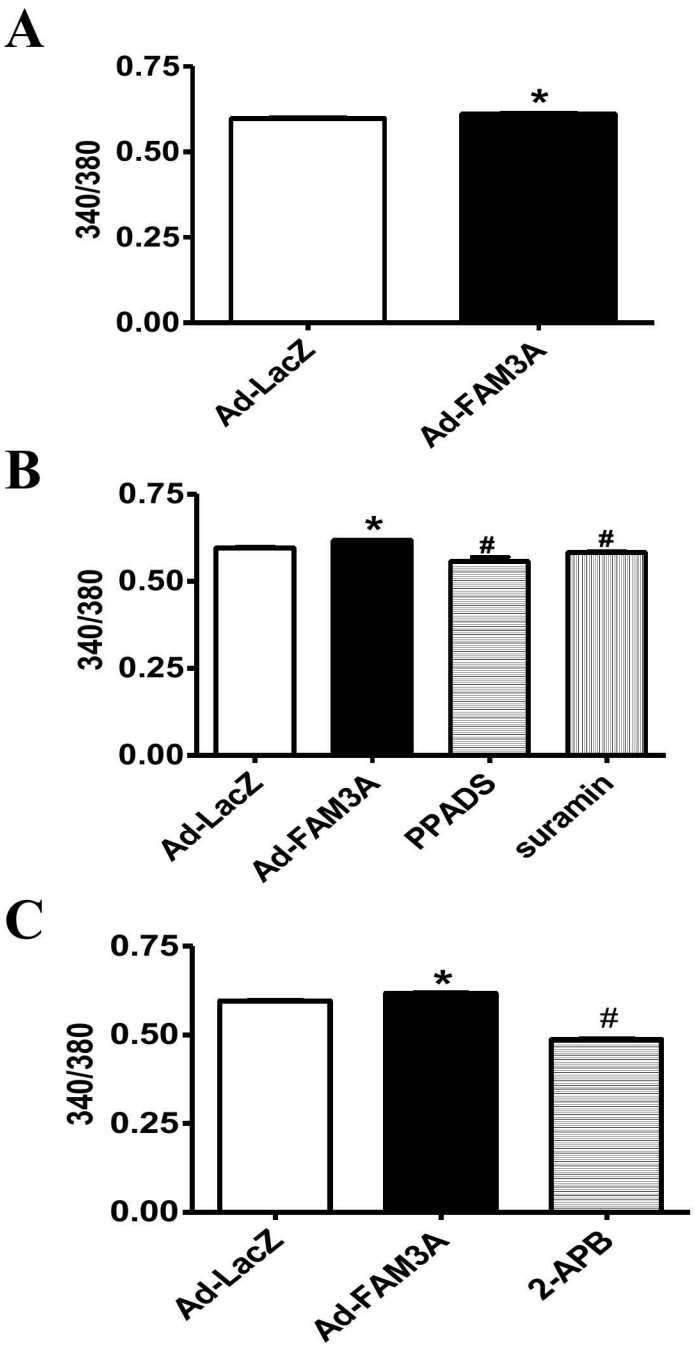

Supplemental Figure 2

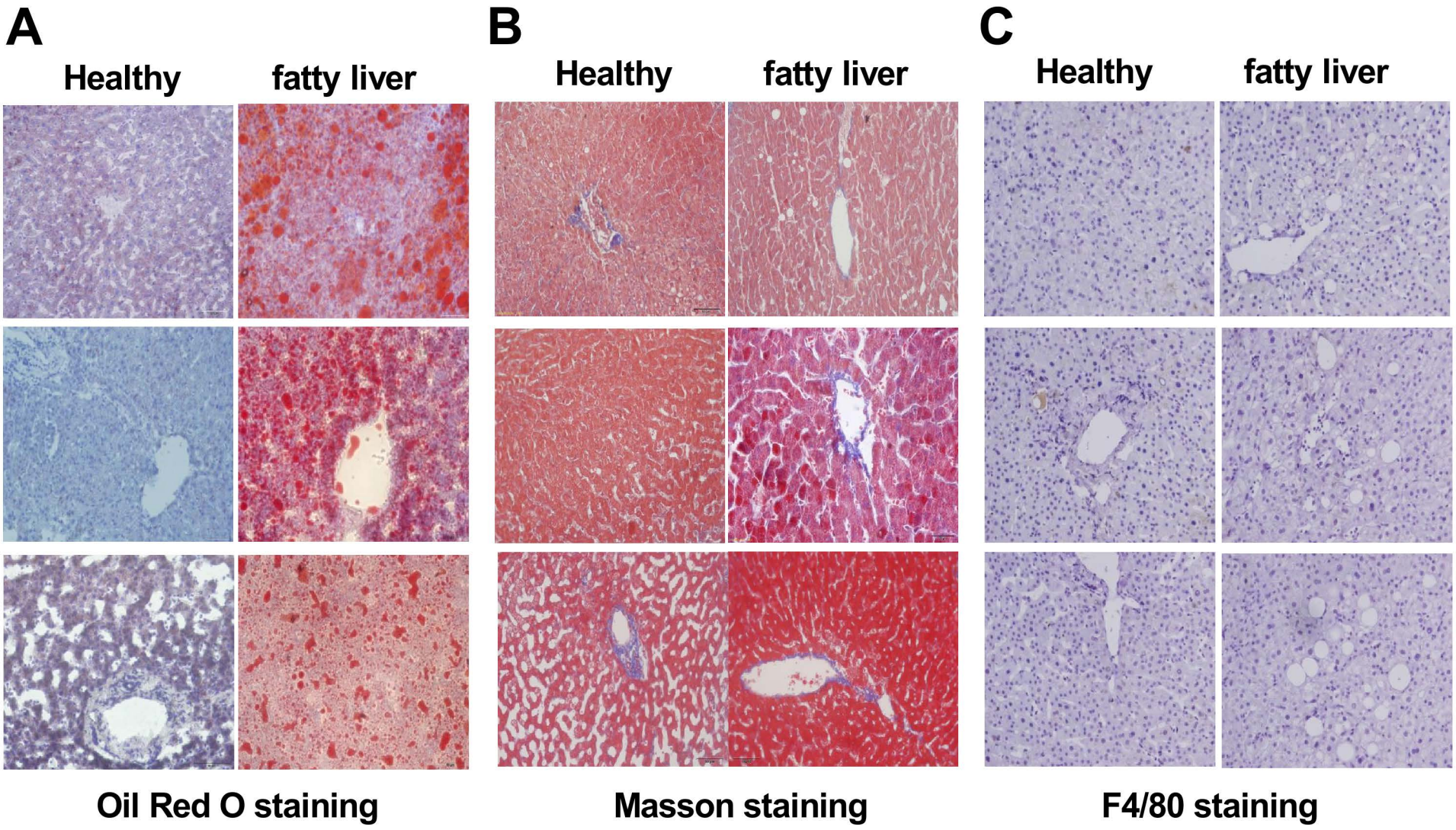

Supplemental Figure 3

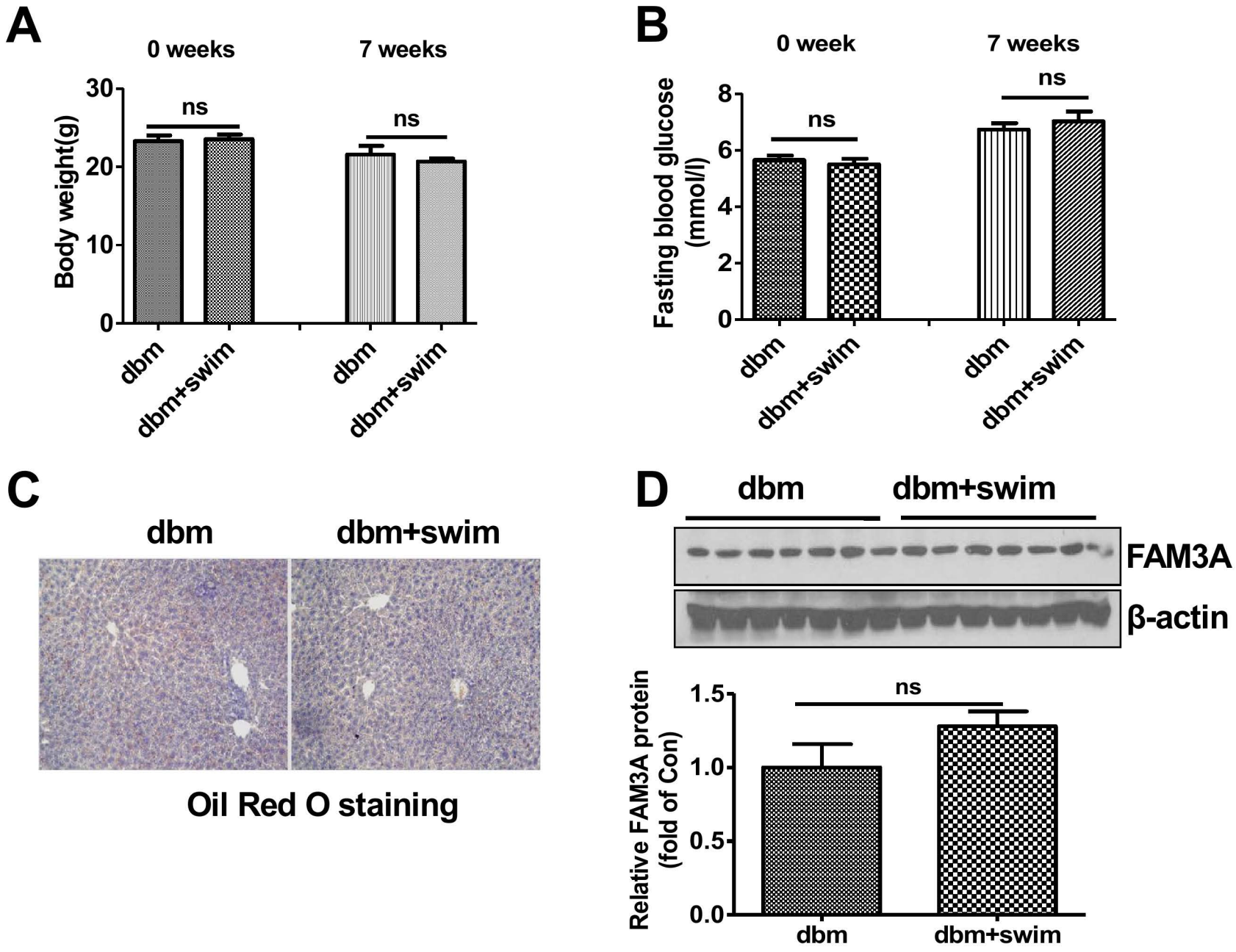

Supplemental Figure 4

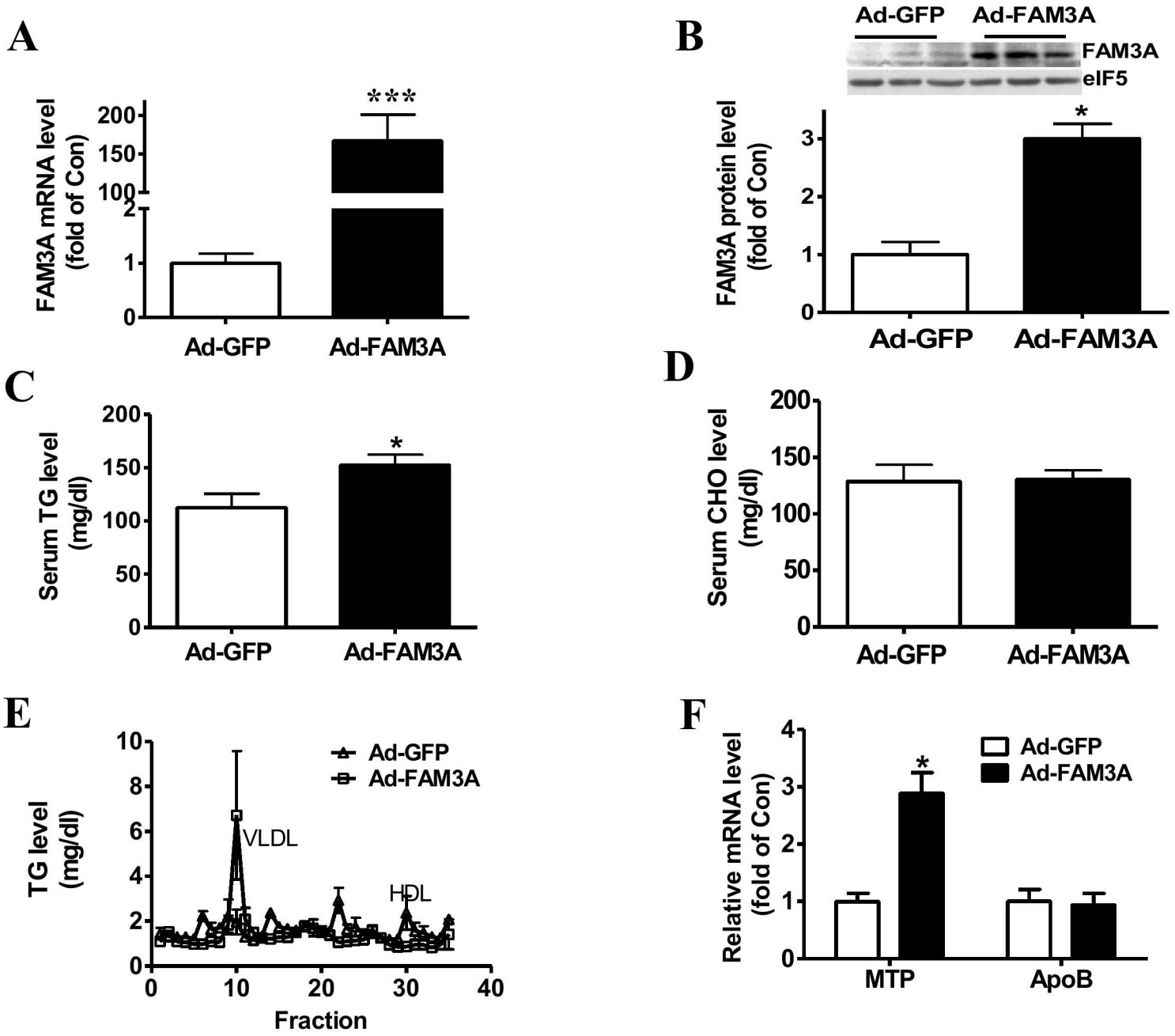

Supplemental Figure 5

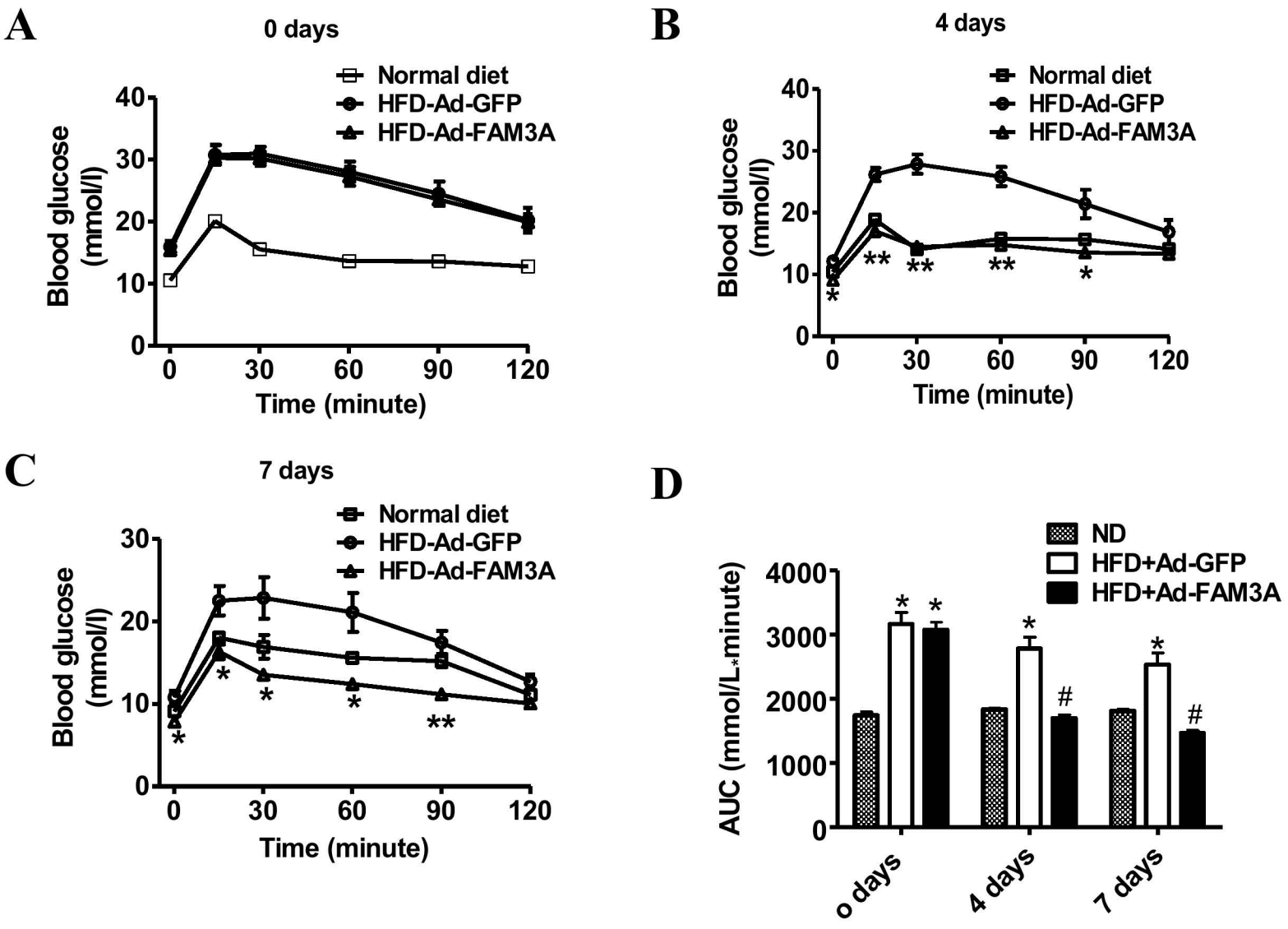

Supplemental Figure 6

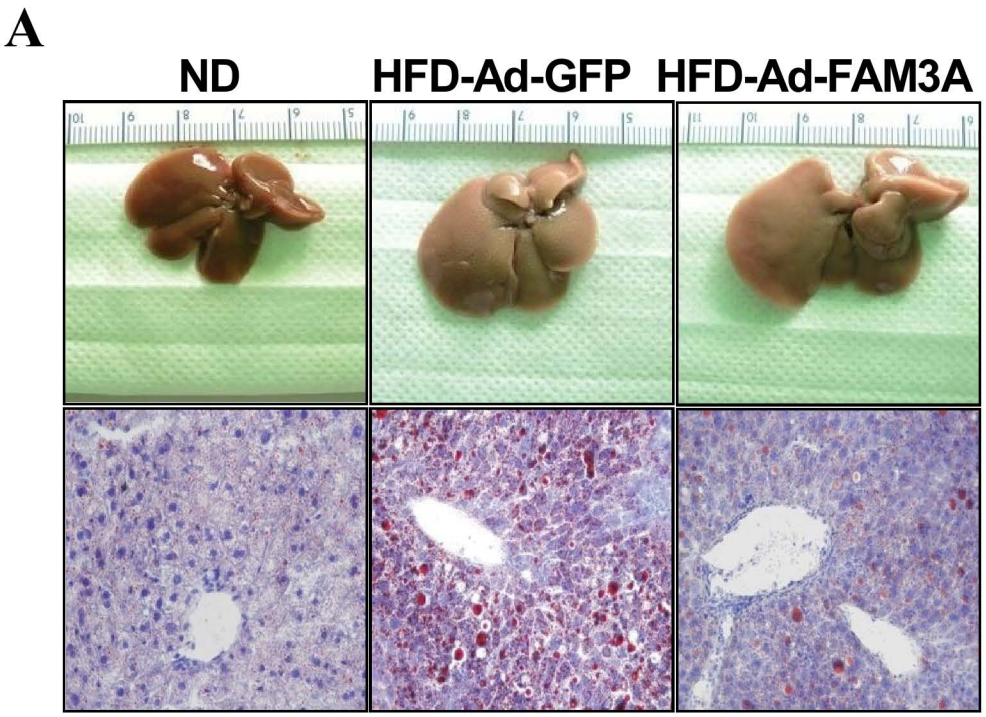

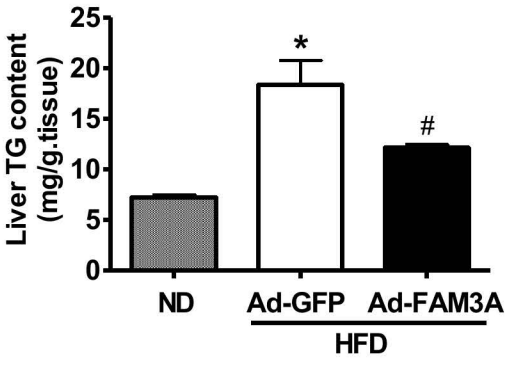

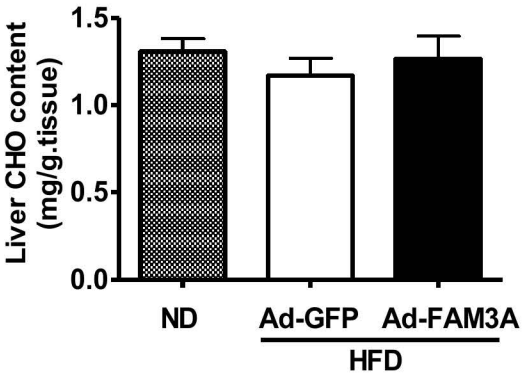

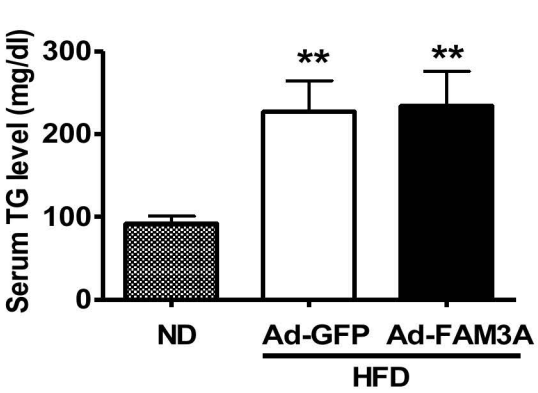

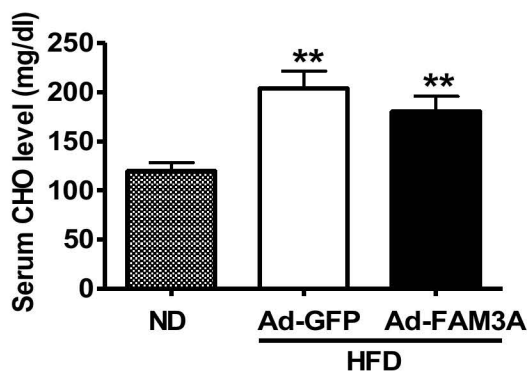

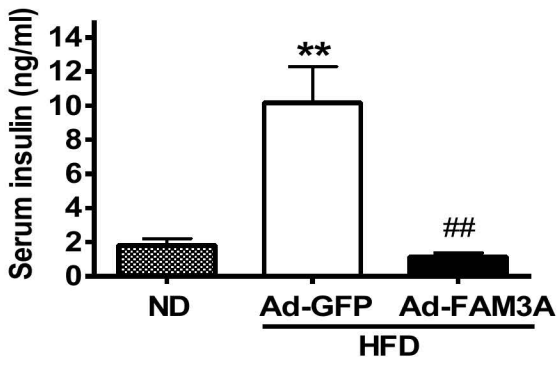

Supplemental Figure 7

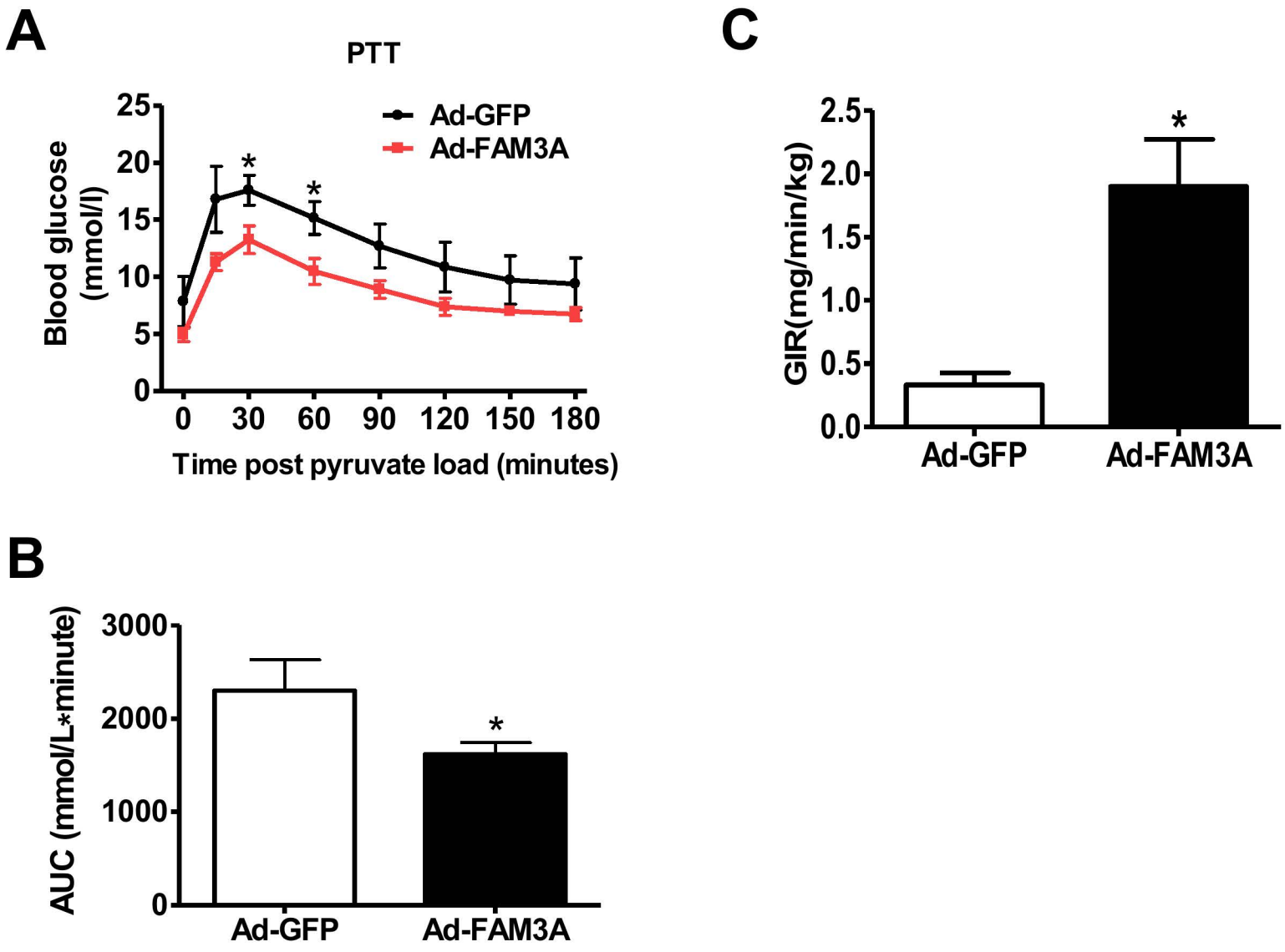

Supplemental Figure 8

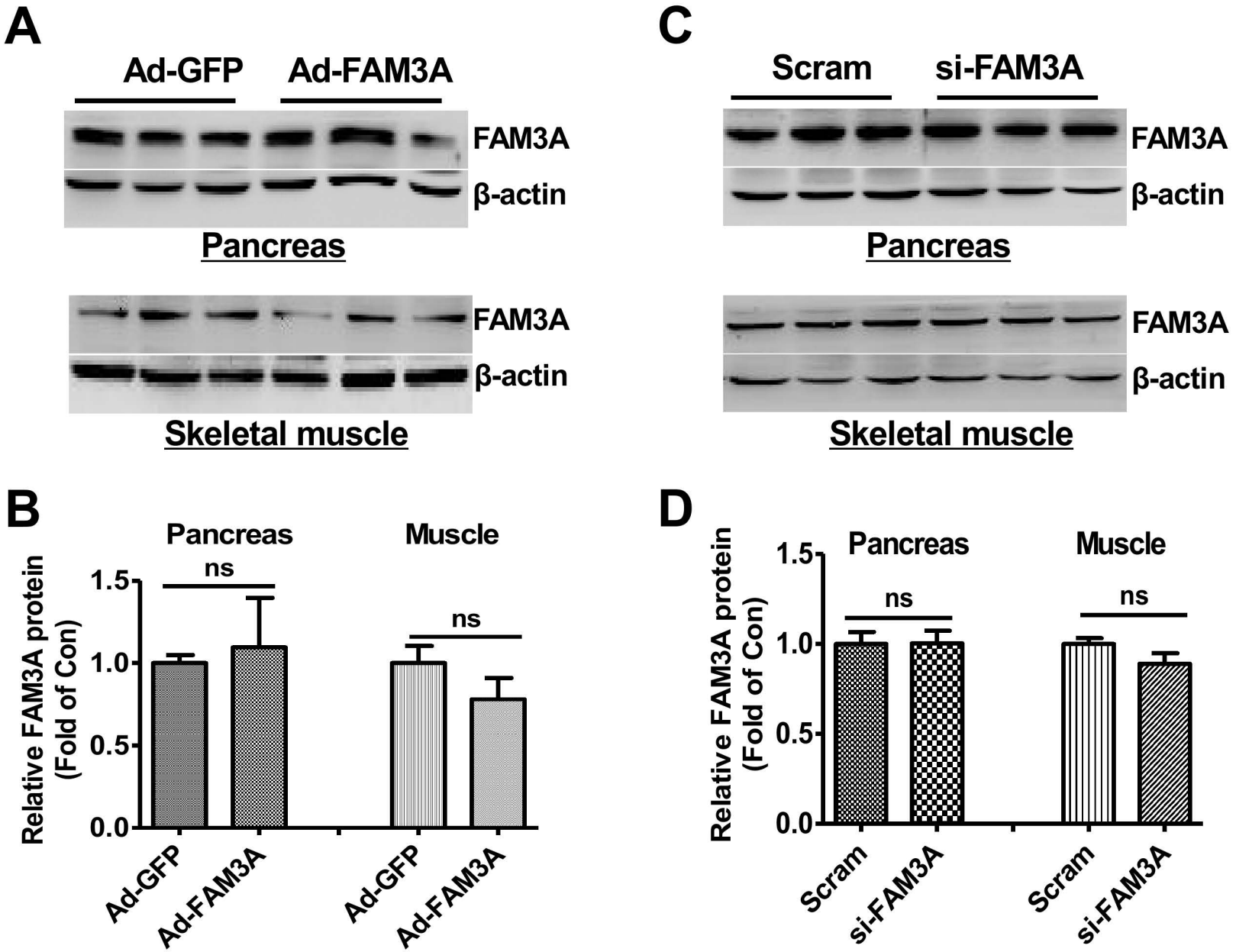

Supplemental Figure 9

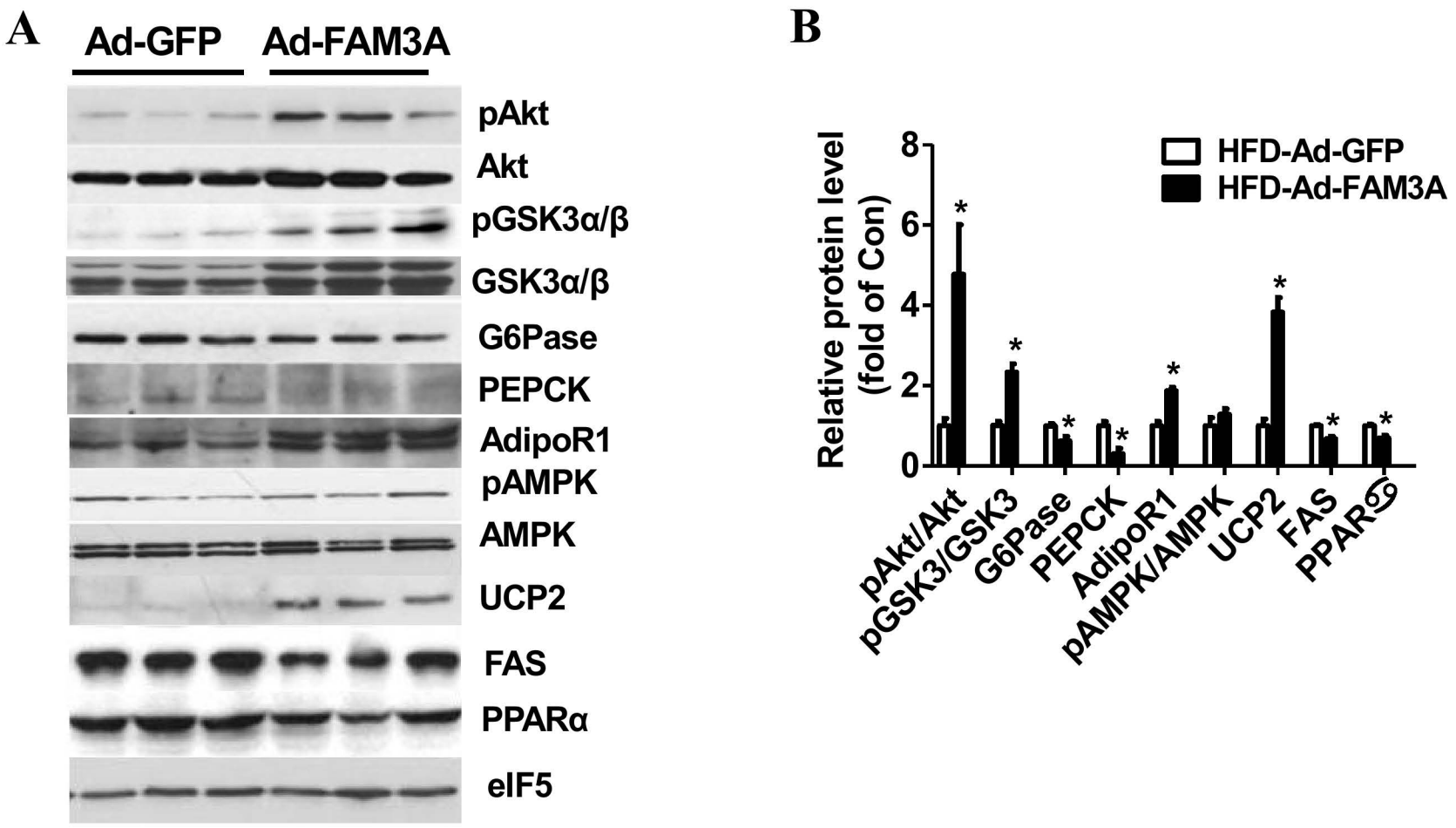

Supplementary experimental procedure

Calcium measurement - HepG2 cells were loaded with 1μM Fura-2 AM for 10 min, and then imaged under Olympus ix71 fluorescence microscope. Emission intensities under 340nm and 380nm illumination were recorded every second, and the ratio of the emission densities (F340/F380) reflects the intracellular free calcium concentration (1). For basal calcium concentration measurements, HepG2 cells were treated with indicated concentrations of U73122, 2-APB, PPADS and suramin for 1 hour. HepG2 cells were also pretreated for 1 hour with U73122, 2-APB, PPADS and Suramin before being incubated with 100μM ATP.

Hyperinsulinemic euglycemic clamp - Hyperinsulinemic euglycemic clamp was performed as described previously (2, 3). In brief, db/db mice infected with Ad-FAM3A or Ad-GFP for 7 days were fasted overnight, and the hyperinsulinemic euglycemic clamp technique was carried out with a prime-continuous infusion of human insulin at a rate of 180 pmol/kg/min. Blood samples were obtained every 10 minutes for determination of blood glucose concentrations, which were maintained at the basal levels by the perfusion of 10% glucose at variable rates for 2 hours.

Pyruvate tolerance tests - The protocol for pyruvate tolerance tests (PTT) was detailed elsewhere (4). In brief, db/db mice infected with Ad-FAM3A or Ad-GFP for 7 days were fasted for 16 hours and were injected intraperitoneally with pyruvate (0.75mg/Kg body weight in saline). Blood glucose levels were measured from the tail

vein at indicated times using a Freestyle brand glucometer.

Collection of human liver samples - Liver samples were obtained from 6 patients who were admitted to Peking University First Hospital, Peking University People's Hospital and Nantong University Affiliated Hospital for diagnosis and treatment of hepatic disease. All 6 cases received liver biopsies. Samples of the liver tissue were fixed in 4% paraformaldehyde, embedded in paraffin, cut, and stained with hema-toxylin and eosin (H&E). We staged the liver histology of patients with NAFLD using H&E staining, Oil red O staining, Masson staining and F4/80 staining assays. The study was conducted under informed consent and approved by the Ethical Committee on Human Research. Some clinical characteristics of the 6 patients are listed in Supplemental Table 2. The study protocol involving human samples conformed to the ethic guidelines of the 1975 Declaration of Helsinki as evidenced by prior approval from the appropriate institutional review committee.

Categorization of simple fatty liver in human liver samples - According to the guidelines proposed for the diagnosis and treatment of nonalcoholic fatty liver diseases for Chinese population, simple fatty liver can be categorized into four degrees, which are designated as F1–F4, respectively (5). F0: hepatocellular steatosis less than 5% (Healthy subjects); F1: hepatocellular steatosis between 5% and 30%; F2: hepatocellular steatosis between 31% and 50%; F3： hepatocellular steatosis between 51% and 75%; F4: hepatocellular steatosis more than 75% (5). In our study, the

simple fatty livers were diagnosed and scored by a board-certified pathologist in the Department of Pathology at Peking University using the guidelines above.

Culture of primary mouse hepatocytes

Five-5-week-old male C57BL/6 mice were anaesthetized with 10% chloral hydrate, and liver was perfused with heparin , solution I, and solution II, respectively as detailed previously (6). The perfused liver was passed though a 400 screening size filter by flushing with RPMI 1640 medium. The hepatocytes were collected by centrifuge at 50g for 2 minutes, re-suspended with 1640 medium and planted in 6-well plates for experimental purposes.

Immunohistochemistry and immunofluorescence

Pancreases and livers were fixed and dehydrated, and embedded in paraffin wax. Immunohistochemical staining procedure has been detailed previously (7). For immunofluorescence assay, HepG2 cells planted on slides were transfected with Mito-DsRed plasmid and ER-DsRed plasmid (kindly provided by Drs. Dalong Ma and YingYu Chen from Peking University) (8, 9) or FAM3A-HA plasmid (GeneCopoeia) for 48 hours, and then the slides were fixed with 4% paraformaldehyde for 15 min and permeabilized with 0.5% Triton X-100 for 10 min. Nonspecific binding was blocked in 1% BSA at room temperature for 10 min, followed by incubation with primary antibody overnight at 4°C. The slides were then incubated with Alexa fluo 488 antibodies or Alexa fluo 594 antibodies (1:200).

Images were obtained using Confocal microscopy.

Mitochondria isolation

Mitochondria were isolated from liver tissue or HepG2 cells using the Mitochondria/Cytosol Fractionation Kit (Pierce) in accordance with the manufacturer's protocol (10). FAM3A protein in isolated mitochondria or cytoplasmic fractions was analyzed by western blot.

References

1. Yang J, Wong RK, Park M, Wu J, Cook JR, York DA, Deng S, et al. Leucine regulation of glucokinase and ATP synthase sensitizes glucose-induced insulin secretion in pancreatic beta-cells. Diabetes 2006;55:193-201.
2. Tao R, Ye F, He Y, Tian J, Liu G, Ji T, Su Y. Improvement of high-fat-diet-induced metabolic syndrome by a compound from Balanophora polyandra Griff in mice. Eur J Pharmacol 2009;616:328-333.
3. Brozinick JT, Jr., McCoid SC, Reynolds TH, Nardone NA, Hargrove DM, Stevenson RW, Cushman SW, et al. GLUT4 overexpression in db/db mice dose-dependently ameliorates diabetes but is not a lifelong cure. Diabetes 2001;50:593-600.
4. Kim KH, Jeong YT, Oh H, Kim SH, Cho JM, Kim YN, Kim SS, et al. Autophagy deficiency leads to protection from obesity and insulin resistance by inducing Fgf21 as a mitokine. Nat Med 2013;19:83-92.
5. Zeng MD, Fan JG, Lu LG, Li YM, Chen CW, Wang BY, Mao YM. Guidelines for the diagnosis and treatment of nonalcoholic fatty liver diseases. J Dig Dis 2008;9:108-112.
6. Wang R, Kong X, Cui A, Liu X, Xiang R, Yang Y, Guan Y, et al. Sterol-regulatory-element-binding protein 1c mediates the effect of insulin on the expression of Cidea in mouse hepatocytes. Biochem J 2010;430:245-254.
7. Li J, Chi Y, Wang C, Wu J, Yang H, Zhang D, Zhu Y, et al. Pancreatic-derived factor promotes lipogenesis in the mouse liver: role of the Forkhead box 1 signaling pathway. Hepatology 2011;53:1906-1916.
8. Yu C, Wang L, Lv B, Lu Y, Zeng L, Chen Y, Ma D, et al. TMEM74, a lysosome and autophagosome protein, regulates autophagy. Biochem Biophys Res Commun 2008;369:622-629.
9. Wang P, Sun B, Hao D, Zhang X, Shi T, Ma D. Human TMEM174 that is highly expressed in kidney tissue activates AP-1 and promotes cell proliferation. Biochem Biophys Res Commun 2010;394:993-999.

10. Liu XD, Sun H, Liu GT. 5-Bromotetrandrine enhances the sensitivity of doxorubicin-induced apoptosis in intrinsic resistant human hepatic cancer Bel7402 cells. Cancer Lett 2010;292:24-31.

Figure legends of supplementary data

Supplemental Figure 1. Tissue distribution of mouse FAM3A and effect of physical exercise on hepatic FAM3A expression in the livers of db/db mice. (A) RT-PCR analysis showing that FAM3A mRNA was ubiquitously expressed in mouse tissues. (**B**) Real-time PCR analysis demonstrating the difference of FAM3A mRNA levels in various tissues between db/m and db/db mice. *p<0.05 *vs.* db/m, n=5. **(C-D)** 7-week swimming exercise increased the mRNA (C) and protein (D) levels of FAM3A in the livers of db/db mice. db/m, db/m mice; db/db, db/db mice; db/db+exer, exercised db/db mice. *P<0.05 *vs.* db/m mice, #P<0.05 *vs.* db/db mice, n=5.

Supplemental Figure 2. **Lipid deposition, fibrosis and inflammation assays of human liver samples**. **(A)** Oil Red O staining assay for determining lipid deposition. **(B)** Masson staining assay for fibrosis analysis. **(C)** F4/80 staining assay for detection of inflammation. F4/80 is the biomarker for liver macrophages. In all staining assays, three healthy liver samples and three fatty liver samples were analyzed.

Supplemental Figure 3. **7-week swimming exercise failed to affect FAM3A expression in the livers of db/m mice.** 8-12 week old male db/m mice were subject to swimming exercise for 45 minutes for 7 weeks. **(A)** Effect of swimming exercise

on body weight of db/m mice**. (B)** Effect of swimming exercise on fasting blood glucose of db/m mice **(C)** Effect of swimming exercise on hepatic lipid deposition of db/m mice as indicated by Oil Red O staining assay. **(D)** Effect of swimming exercise failed to affect FAM3A protein levels in the livers of db/m mice. The data were presented as mean ± SE of 7 mice. NS, no significant difference between two groups.

Supplemental Figure 4. Hepatic overexpression of FAM3A increased serum VLDL-TG levels in db/db mice. **(A-B)** Ad-FAM3A treatment significantly increased the mRNA (A) and protein (B) levels of FAM3A in the livers of db/db mice. **(C)** Effect of hepatic FAM3A overexpression on serum levels of TG in db/db mice. **(D)** Effect of hepatic FAM3A overexpression on serum levels of CHO in db/db mice. **(E)** Hepatic FAM3A overexpression increased serum VLDL-TG levels in db/db mice. **(F)** Hepatic FAM3A overexpression increased the mRNA level of MTP. Lipid profile was measured as described in the experimental procedure. TG, triglyceride; CHO, cholesterol. MTP, microsomal triglyceride transfer protein. ApoB, apolipoprotcin B.

*P<0.05 & ***P<0.001 *vs.* the control mice treated with Ad-GFP, n=5-8.

Supplemental Figure 5. Hepatic overexpression of FAM3A significantly ameliorated hyperglycemia in high-fat diet-induced diabetic mice. 6-8 week old male C57BL/6 were fed with a high-fat diet for 12 weeks before viral injection. **(A)** OGTT test in mice fed with HFD for 12 weeks without Ad-GFP or Ad-FAM3A injection. **(B)** OGTT test in mice at 4th day post Ad-GFP or Ad-FAM3A injection,

respectively. **(C)** OGTT test in mice receiving Ad-GFP or Ad-FAM3A treatment for 7 days. **(D)** AUCs for OGTT data shown in A-C. ND: mice fed with a normal diet; HFD: mice fed with a high-fat diet. *P<0.05 & **P<0.01 *vs.* HFD-fed mice treated with Ad-GFP, n=10.

Supplemental Figure 6. Hepatic Overexpression of FAM3A ameliorated fatty liver in HFD-treated mice. C57Bl/6 mice were fed with HFD for 12 weeks and then injected Ad-GFP or Ad-FAM3A via tail vein. At 8^{th} day post virus injection, the mice were sacrificed and tissues and serum were collected for experimental assays. **(A)** Morphological and Oil Red O staining assays revealed a significant reduction of hepatic lipid contents after FAM3A overexpression. **(B)** Quantitative measurements of the TG contents in Ad-GFP treated- and Ad-FAM3A-treaed livers. **(C)** Liver CHO content was not significantly altered by FAM3A overexpression. **(D-E)** Hepatic overexpression of FAM3A had little effect on serum TG (D) and CHO (E) levels. **(F)** Serum insulin levels were markedly reduced in mice with hepatic FAM3A overexpression. *P<0.05 & **P<0.01 *vs.* normal diet (ND) mice; #P<0.05 & ##P<0.01 *vs.* HFD-fed mice treated with Ad-GFP, respectively, n=10.

Supplemental Figure 7. **FAM3A overexpression improved global insulin sensitivity and suppressed hepatic glucose production in db/db mice.** Seven days post Ad-FAM3A or Ad-GFP injection, the mice were subject to pyruvate tolerance test and hyperinsulinemic euglycemic clamp assay. **(A)** Pyruvate tolerance test (PTT) of

db/db mice with FAM3A overexpression. **(B)** Area under curve (AUC) of PTT data shown in (A). **(C)** Hyperinsulinemic euglycemic clamp assay of db/db mice with FAM3A overexpression. The data were presented as mean ± SE of 5 mice. *P<0.05 *vs.* Ad-GFP-treated mice, n=5.

Supplemental Figure 8. **Adenovirus or siRNA injection had little effect on FAM3A protein levels in skeletal muscle and the pancreas of mice. (A-B)** Ad-FAM3A treatment failed to affect FAM3A protein level in the muscle and pancreas of db/db mice. The representative gel images were shown in (A), and quantative data shown in (B). **(C-D)** si-FAM3A treatment failed to affect FAM3A protein levels in the muscle and pancreas of normal mice. The representative gel images were shown in (C), and quantative data shown in (D)**.** The data were presented as mean ± SE of 5 mice. NS, no significant difference between two groups.

Supplemental Figure 9. Effect of FAM3A overexpression on protein levels of genes involved in glucose and lipid metabolism in the livers of HFD-treated mice. (A) FAM3A overexpression resulted in a significant increase in pAkt, pGSK3a/b, AdipoR1, and UCP2 levels and a marked decrease in expression levels of gluconeogenic gene G6Pase and PEPCK and lipogenic gene FAS in the livers of HFD-fed mice. **(B)** Quantitative measurements of protein expression levels of genes shown in (A). *P<0.05 *vs.* control mice infected with Ad-GFP, n=5-8.

Supplemental Figure 10. siRNA-mediated knockdown of hepatic FAM3A gene reduced the mRNA and protein levels of FAM3A in the livers of C57BL/6 mice. **(A)** siFAM3A treatment significantly reduced FAM3A mRNA expression. **(B)** Hepatic FAM3A gene knockdown resulted in a marked reduce in FAM3A protein levels in the livers of C57BL/6 mice. **(C)** Hepatic FAM3A gene knockdown elevated the mRNA levels of CD36 and ELOVL6. **(D)** Hepatic FAM3A gene knockdown elevated the protein level of CD36. The mice were received siFAM3As or scrambled siRNAs as described in the experimental procedure. *P<0.05 & **P<0.01 *vs.* mice treated with scrambled siRNAs, n=5.

Supplemental Figure 11. Effect of FAM3A on the association of IRS-1 with PI3K in liver cells. (A) FAM3A had little effect on the association of IRS-1 with the p85 sununit of PI3K in HepG2 cells. HepG2 cells were treated with Ad-FAM3A or Ad-GFP for 48 hours and then stimulated with or without insulin (100nM) for 5min. CoIP assay was performed with anti-IRS-1 antibody and pIRS-1, p85 and IRS-1 were tested by immunobloting. n=5. IP: immunoprecipitation; IB: immunobloting. **(B)** Little effect of FAM3A on the association of IRS-1 with the p85 subunit of PI3K in the livers of db/db mice, n=5. **(C)** FAM3A activated Akt independent of insulin in primary cultured mouse hepatocytes. pAkt level was increased in primary cultured mouse hepatocytes treated with Ad-FAM3A for 36 hours in the absence of insulin stimulation. *P<0.05 *vs.* control hepatocytes infected with Ad-GFP, n=4. **(D)** Ad-FAM3A treatment had no effect on PTEN, p110α and p110β expression in HepG2

cells in the presence or absence of insulin treatment (100 nM for 5 minutes), n=3. **(E)** FAM3A overexpression did not alter the protein levels of PTEN, p110α and p110β in the livers of db/db mice. n=5.

Supplemental Figure 12. Hepatic overexpression of FAM3A attenuated hyperglycemia in STZ-induced type 1 diabetic mice. 8-week old male C57BL/6 mice were induced hyperglycemia via STZ injection (50mg/kg/day for 5 days). One month after STZ injection, the mice with blood glucose levels over 18 mM were chosen for experiments. $0.8x10^9$ pfu of Ad-FAM3A or Ad-GFP were injected into the mice via tail vein. Fasting blood glucose levels were monitored 4 days and 7 days after the virus injection. **(A)** Hepatic FAM3A overexpression attenuated fasting blood glucose levels in STZ-treated mice. **(B)** Western blot analysis showing the effect of FAM3A on Akt activation, gluconeogenic gene expression and AdipoR1 and UCP2 expression in the livers of STZ-induced diabetic mice receiving either Ad-GFP or Ad-FAM3A treatment. **(C)** Quantitative measurement of the expression levels of the proteins shown in (B). **(D)** Hepatic FAM3A overexpression significantly reduced the mRNA levels of gluconeogenic G6Pase and PEPCK. *P<0.05 & **P<0.01 *vs.* STZ-induced diabetic mice treated with Ad-GFP, n=6.

Supplemental Figure 13. FAM3A was located mainly in the mitochondria and endoplasmic reticulum. (A-B) HepG2 cells were transfected with the Mito-DsRed plasmids (A) and ER-DsRed plasmids (B), and immunofluorescence was performed

using anti-FAM3A antibody. **(C-D)** HepG2 cells were transfected with FAM3A-HA plasmids and the Mito-DsRed plasmids (C) and ER-DsRed plasmids (D). Then immunofluorescence was performed using anti-HA antibody. The images shown were the representatives of at least 5 independent experiments. **(E-F)** FAM3A protein was detected in isolated mitochondria of HepG2 cells (E) and mouse livers (F). **(G)** Ad-FAM3A treatment resulted in increased FAM3A protein in isolated mitochondria of db/db mouse livers (n=4). **(H)** Ad-FAM3A infection elevated cellular FAM3A protein level in HepG2 cells. No FAM3A protein was detected in the medium of Ad-FAM3A-treated HepG2 cells. The images shown were the representatives of at least 3 independent experiments. Mito, mitochondria; ER: endoplasmic reticulum; cyto, cytoplasmic fraction.

Supplemental Figure 14. Exogenous ATP activated Akt through the PI3K p110α in HepG2 cells. **(A)** Exogenous ATP activated Akt via the PI3K p110α-dependent pathway in HepG2 cells**.** HepG2 cells were pretreated with wortmannin (1 μM), p110α inhibitor PIK 75 (100 nM) or DMSO for 30min followed by the treatment with 100 μM ATP for 5min. *P<0.05 *vs.* Con; #P<0.05 *vs.* D; n=5. Con: Control; D: DMSO-treated cells in the presence of ATP; W: wortmannin; PIK75: p110α inhibitor. **(B)** ATP-induced Akt activation was blocked by the P2 receptor antagonist PPADS. HepG2 cells were pretreated with PPADS (50 μM) for 1 hour before the treatment with 100 μM ATP for 5min. *P<0.05 *vs.* Con; #P<0.05 *vs.* ATP-treated cells; n=5. **(C-D)** ATP increased cytosolic free calcium levels in HepG2 cells, which was

attenuated by the pretreatment with the PLC inhibitor U73122 (5 μM) (C) and the IP3R antagonist 2-APB (D) (50 μM) for 1 hour. The data were presented as mean ± SE of at least 300 cells in at least 5 independent experiments. **(E)** Suramin dose-dependently inhibited FAM3A-induced Akt activation in HepG2 cells. Ad-FAM3A-infected HepG2 cells were treated with the indicated concentrations of suramin for 1 hour before pAkt were assayed. *P<0.05 *vs.* Ad-GFP-treated cells; #P<0.05 *vs.* Ad-FAM3A-infected cells without suramin treatment, n=5.

Supplemental Figure 15. **FAM3A elevated cytosolic free calcium levels in HepG2 cells via the P2 receptors. (A)** FAM3A overexpression significantly increased cytosolic free calcium levels. Ad-LacZ infected cells as control. **(B)** Pretreatment with the P2 receptor antagonist PPADS (50 μM) or suramin (50 μM) for 1 hour repressed FAM3A-induced increase in cytosolic free calcium levels. **(C)** Pretreatment with the IP3R antagonist 2-APB (50 μM) for 1 hour suppressed FAM3A-induced increase in cytosolic free calcium levels. The data were presented as mean ± SE of at least 300 cells in at least 5 independent experiments, *P<0.05 *vs.* Ad-LacZ-infected cells; #P<0.05 *vs.* Ad-FAM3A-treated cells.

Table 1. List of oligonucleotide primer pairs used in real time RT-PCR and RT-PCR analysis, and for cloning the promoter fragment of human and mouse *FAM3A* genes.

M: mouse; R: rat; H: human. If not indicated, all the primer sequences are referred to mouse orgin.

Target Gene	Sense Primer	Antisense Primer
G6Pase	5'-AGGAAGGATGGAGGAAGGAA-3'	5'-TGGAACCAGATGGGAAAGAG-3'
PEPCK	5'-ATCTTTGGTGGCCGTAGACCT-3'	5'-CCGAAGTTGTAGCCGAAGAA-3'
GK	5'-TATGAAGACCGCCAATGTGA -3'	5'-CACTGAGCTCTCATCCACCA -3'
β-actin	5'-AGCCATGTACGTAGCCATCC -3'	5'-GCTGTGGTGGTGAAGCTGTA -3'
FAM3A (M)	5'-TCATGAGCAGCGTCAAAGAC-3'	5'-AGGGTACCTTCATGCAGTGG-3'
FAM3A (H)	5'-GTGTCACATGGATCGTGGTC-3'	5'- TGCTCAATCAGCATCTTGTCC-3'
MTP	5'-AACTCCTACGAGCCCTCCTT-5'	5'-AGTCCTCCCAGGATCAGCTT-3'
ApoB	5'-TCACCATTTGCCCTCAACCTAA-3'	5'-GAAGGCTCTTTGGAAGTGTAAAC-3'

Table 2. Clinical characteristics of human subjects with or without NALFD

	Patient NO.	Height (cm)	Weight (kg)	BMI	comorbidities	ALT (U/L)	AST (U/L)	gender	Degree of steatosis	fibrosis	inflammation
Normal	1	165	62	22.77	-	16	28	male	FO	-	-
	2	172	65	21.97	hypertension	13	21	male	FO	-	-
	3	174	60	19.82	-	12	14	female	FO	-	-
NAFLD	1	173	108	36.09	Hypertension Dyslipidemia	12	17	male	F3	-	-
	2	172	80	27.04	Dyslipidemia	14	25	male	F4	-	-
	3	176	75	24.21	hypertension	42	28	female	F3	-	-